

Controlled Polymerization of Norbornene Cycloparaphenylenes Expands Carbon Nanomaterials Design Space

Ruth L. Maust, Penghao Li, Baihao Shao, Sarah M. Zeitler, Peiguan B. Sun, Harrison W. Reid, Lev N. Zakharov, Matthew R. Golder, and Ramesh Jasti*



Cite This: *ACS Cent. Sci.* 2021, 7, 1056–1065



Read Online

ACCESS |



Metrics & More



Article Recommendations



Supporting Information

ABSTRACT: Carbon-based materials—such as graphene nanoribbons, fullerenes, and carbon nanotubes—elicit significant excitement due to their wide-ranging properties and many possible applications. However, the lack of methods for precise synthesis, functionalization, and assembly of complex carbon materials has hindered efforts to define structure–property relationships and develop new carbon materials with unique properties. To overcome this challenge, we employed a combination of bottom-up organic synthesis and controlled polymer synthesis. We designed norbornene-functionalized cycloparaphenylenes (CPPs), a family of macrocycles that map onto armchair carbon nanotubes of varying diameters. Through ring-opening metathesis polymerization, we accessed homopolymers as well as block and statistical copolymers constructed from “carbon nano-hoops” with a high degree of structural control. These soluble, sp^2 -carbon-dense polymers exhibit tunable fluorescence emission and supramolecular responses based on composition and sequence. This work represents an important advance toward bridging the gap between small molecules and functional carbon-based materials.



INTRODUCTION

The versatility of carbon nanomaterials makes them extremely useful. From graphitic structures such as carbon nanotubes and fullerenes, which have become indispensable in electronics,^{1,2} to carbon quantum dots with tunable fluorescence,³ carbon materials have emerged as promising candidates for a wide range of applications. The utility of carbon nanomaterials for various end uses ultimately depends on how well their properties can be fine-tuned. Currently, many carbon materials are prepared through uncontrolled processes, resulting in poorly defined products and hindering the design of new materials based on structure–property relationships. In recent years, significant progress has been made in synthesizing molecular nanocarbons with new geometries, functionalities, and properties,^{4–6} as well as employing polymer chemistry as a means to access useful carbon-based materials.^{7–11} Major challenges remain, however; the majority of syntheses of extended carbon structures rely on lengthy synthetic sequences—often impeded by substrate insolubility, tedious purification steps, and low yields—or uncontrolled, step-growth polymerization methods. Notwithstanding notable exceptions,^{12–15} the connectivities and functionalities accessible via well-controlled methods remain limited.

To address these challenges, we envisioned that a family of oligomeric nanocarbons—cycloparaphenylenes—could serve as the basis for constructing larger, structurally-defined carbon materials using controlled polymerization. Cycloparaphenylenes (CPPs) are atomically precise cyclic oligomers, and, like discrete linear oligomers,¹⁶ each CPP size exhibits unique

properties.¹⁷ In addition to changing the number of phenyl rings, the properties of CPPs can also be influenced by incorporating a *meta* linkage,¹⁸ a donor–acceptor motif,¹⁹ or other structural modifications. The cyclic architecture of CPPs makes them especially exciting building blocks for materials. Other classes of macrocycles have previously been shown to impart improved solubility,²⁰ enhanced physical properties,^{21,22} capabilities for guest uptake,^{23–25} and opportunities for varied topology^{26–29} in polymeric materials. CPPs share these desirable traits with other macrocycles^{30–35} and offer an additional advantage over most other macrocycles in that they can be synthesized and functionalized in a completely modular way.

While CPP-based polymers have previously been prepared via cross-coupling polymerization,^{36,37} constructing polymers from CPPs would be especially powerful using controlled or “living” polymerization techniques. Controlled chain-growth polymerization enables synthesis of block copolymers, opening the door to self-assembly and complex hierarchical structures.³⁸ The ability to control polymer chain length and to prepare block copolymers also provides access to materials which arise from the same monomers but possess different

Received: March 17, 2021

Published: May 13, 2021



properties. For this study, we selected ring-opening metathesis polymerization (ROMP) as a route that would not present unwanted modes of reactivity with CPPs, which can undergo strain-relieving reactions not seen in linear aromatic molecules.^{39,40} ROMP, particularly with Ru-based initiators, is known for being well-controlled and highly tolerant of a variety of functional groups.^{41–43} We first sought to demonstrate that ROMP could be used to polymerize all-carbon CPP monomers, with the hopes that this strategy will be applicable to functionalized CPP monomers in the future (Figure 1).

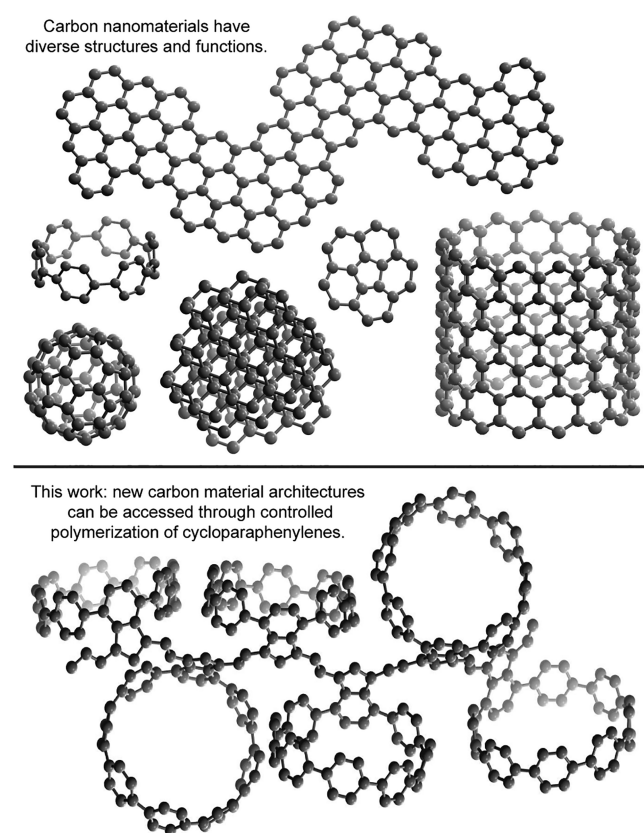


Figure 1. Combining synthetic organic and polymer chemistry approaches can lead to carbon materials with new properties.

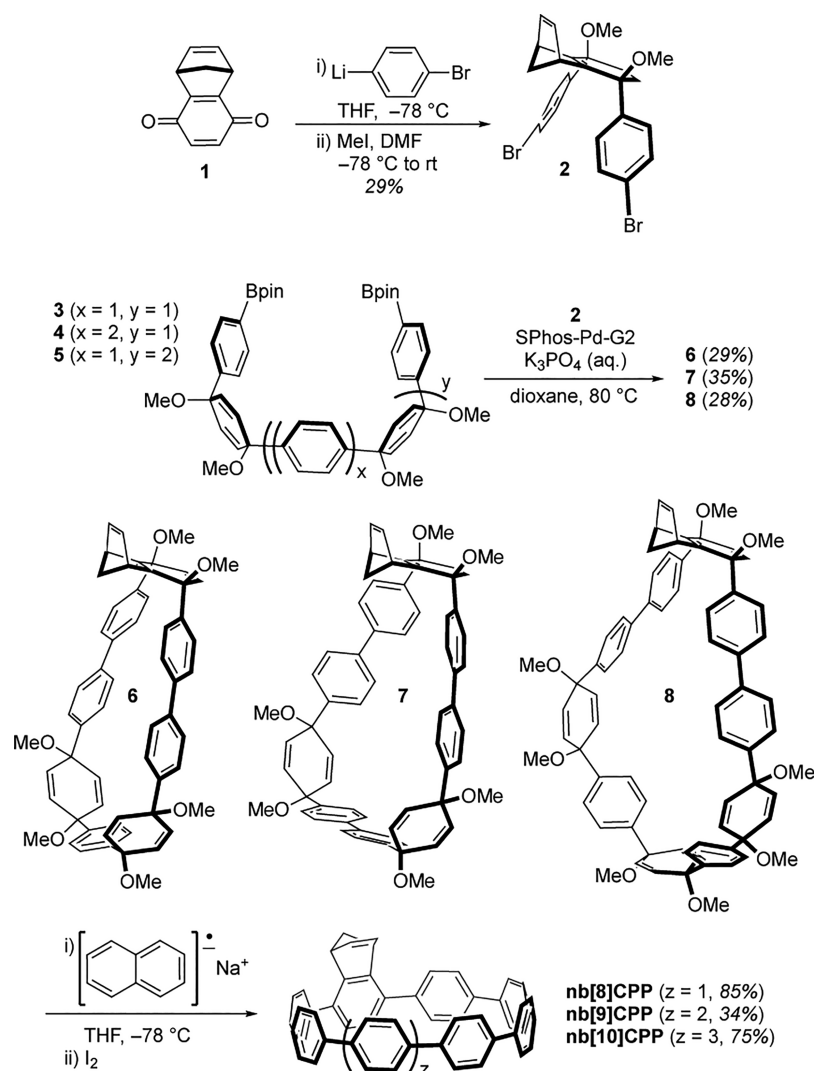
Here we describe the synthesis and characterization of a series of norbornene CPP monomers (**nb[8]CPP**, **nb[9]CPP**, and **nb[10]CPP**) and show their controlled polymerization via ROMP. This approach generated homopolymers with precise cyclic side chains of varying sizes as well as block and statistical copolymers comprising CPP units of two different sizes. The resultant polymers were studied using a variety of methods to gain insight into the degree of control over the polymerization and to begin to unravel structure–property relationships for this new class of carbon materials. In particular, we found that poly(**nbCPP**) homopolymers largely retain the fluorescence properties of the constituent monomers, but to our surprise, block and statistical copolymers with the same composition exhibited divergent fluorescence emissions. Likewise, both composition and sequence played a role in the fluorescence response of poly(**nbCPP**)s to C_{60} addition. To conclude, we offer ideas for further materials development based on these findings.

RESULTS AND DISCUSSION

Synthesis and Structural Characterization of Norbornene CPP Monomers and Poly(nbCPP**)s.** Our general synthetic strategy toward CPPs hinges on the use of cyclohexadienes as masked phenylenes.³⁰ These cyclohexadiene units provide the curvature necessary to carry out the macrocyclization step and can be aromatized at the end of the synthetic sequence. Incorporation of a ROMP-reactive benzonorbornadiene unit in the CPP backbone was readily accomplished using this approach (Scheme 1). Norbornene-benzoquinone **1** was selected as a functionalized cyclohexadiene-containing precursor. Double nucleophilic addition of (4-bromophenyl)lithium to **1** followed by *in situ* methylation of the resulting alkoxides yielded dibromide **2**. This curved intermediate served as a common coupling partner for forming multiple sizes of norbornene CPPs in a modular manner. Norbornene CPP monomers with 8, 9, and 10 phenyl rings were targeted by varying the length of the unfunctionalized coupling partner. Bisboronate coupling partners **3**, **4**, and **5** were prepared by iterative diastereoselective nucleophilic additions and cross-coupling reactions (see SI). These coupling partners were subjected to dilute Suzuki–Miyaura cross-coupling conditions with **2** to obtain macrocycles **6**, **7**, and **8**, respectively. Finally, reductive aromatization of these macrocycles yielded the desired monomers: **nb[8]CPP**, **nb[9]CPP**, and **nb[10]CPP**. ^1H NMR spectra of these monomers show distinct signals for the protons on and around the benzonorbornadiene unit, with the remaining protons on the nanohoop backbone appearing as one overlapping peak with the chemical shift dependent on nanohoop size (Figure S1). Monomer structures were confirmed using X-ray crystallography (see SI). The ease of appending a norbornene group onto CPPs in this manner indicates that this approach could also be effective for synthesizing polymerizable versions of CPPs containing heteroatoms and of other CPP derivatives.

With this series of norbornene CPPs in hand, we turned to investigating the polymerization of these compounds. We screened a range of ROMP conditions and evaluated the success of the polymerizations based on the conversion of monomer to polymer and the resultant polymer dispersity. Conversion was estimated using routine ^1H NMR spectroscopy to compare the size of polymer peaks to the peaks from residual monomer, if any, and dispersity was determined using gel permeation chromatography (GPC) with a refractive index (RI) detector. We found that we could obtain poly(**nb[8]CPP**), poly(**nb[9]CPP**), and poly(**nb[10]CPP**) under a variety of conditions (Figure 2a and Tables S1 and S2). For instance, polymerizations of **nb[8]CPP** were conducted successfully in tetrahydrofuran (THF), dichloromethane (DCM), and chloroform, with the reactions in chloroform providing the lowest measured dispersity values. Subjecting **nb[10]CPP** to Grubbs G1 did not produce any polymer, but both Grubbs G2 and bromopyridyl Grubbs G3 were effective in initiating polymerization. Except in instances where the polymerization reactions did not go to completion and peaks were still visible from the residual monomer, NMR spectra for each polymer type looked identical regardless of reaction conditions, indicating that the resultant polymers had the same backbone structure. In each case, the ^1H NMR spectra of the polymers showed broadening of the overlapping peak from the protons on the nanohoop backbone as well as the appearance

Scheme 1. Key Steps for Synthesizing nb[8]CPP, nb[9]CPP, and nb[10]CPP Monomers



of extremely broad peaks centering around 6.66, 5.65, and 4.37 ppm (Figure 2b and Figure S1). However, the complex stereochemical environment due to many possible orientations of the CPP side chains around the polymer backbone limited the amount of structural information available from NMR spectroscopy. To further verify formation of the desired polymer products, we obtained matrix-assisted laser desorption ionization (MALDI) mass spectra of samples of poly(nb[8]CPP) and poly(nb[10]CPP). Disproportionately high intensity in the lower m/z range prevented determination of the average molecular weights of the samples from the MALDI spectra, but we did observe uniform peak spacing corresponding to the mass of the repeat units (Figure S2), confirming that the CPP structures remained intact during ROMP. Samples referenced hereafter in the main text were prepared in chloroform with Grubbs G3 as the initiator, and comparable results from samples prepared in THF can be found in the SI.

Once it was clear that nb[8]CPP, nb[9]CPP, and nb[10]CPP undergo ROMP as expected, we next addressed the question of “livingness” of the polymerizations in more detail. Although few polymerizations meet the strictest definition for “living” polymerizations,⁴⁴ the key capabilities of practical importance are attaining a range of molecular weights in a predictable manner, achieving dispersity values

suitable for the intended application, and synthesizing block copolymers. We were able to demonstrate these attributes in the synthesis of poly(nbCPP)s, showing that the polymerization is well-controlled, if not entirely “living”. By varying the monomer-to-initiator ratio, we targeted several different molecular weights for poly(nb[8]CPP), poly(nb[9]CPP), and poly(nb[10]CPP), focusing mostly on poly(nb[8]CPP) and poly(nb[10]CPP). When analyzing GPC_{RI} results from these polymerizations, we noticed dramatic differences between the theoretical molecular weights based on monomer-to-initiator ratios and the measured molecular weight values (versus polystyrene standards, see Figure S3). These discrepancies indicated that although polystyrene is routinely used as a standard for molecular weight measurements of many types of polymers, it exhibits significantly different solution-state conformation and/or interactions with GPC column materials than poly(nbCPP)s, so these molecular weight results should be considered primarily as relative values. Despite this caveat, we were able to establish linear relationships between the monomer-to-initiator ratios and the measured molecular weights for samples of poly(nb[8]CPP), poly(nb[9]CPP), and poly(nb[10]CPP) (Figure 3). Dispersity values for these samples ranged from 1.08 to 1.56, with no apparent relationship to degree of polymerization

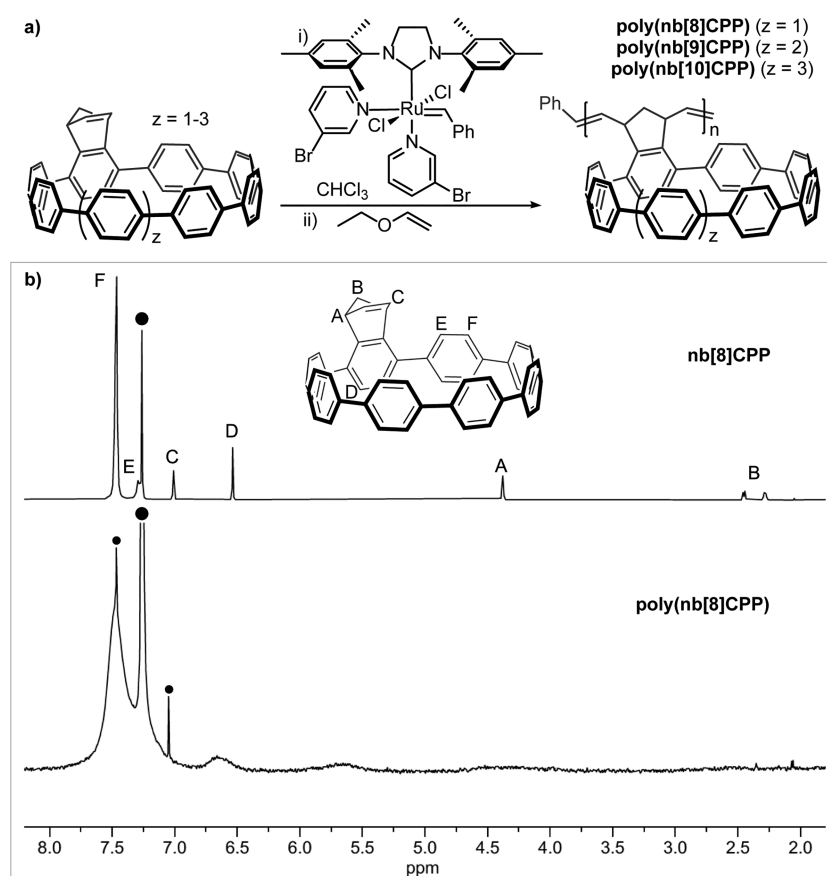


Figure 2. (a) Polymerization of nbCPP monomers under ROMP conditions. (b) Stacked ¹H NMR spectra of nb[8]CPP and poly(nb[8]CPP) (spectrum from sample 4, Table S1). CHCl₃ and its satellite peaks are marked with circles. The peak labeled F corresponds to all CPP backbone protons not otherwise assigned.

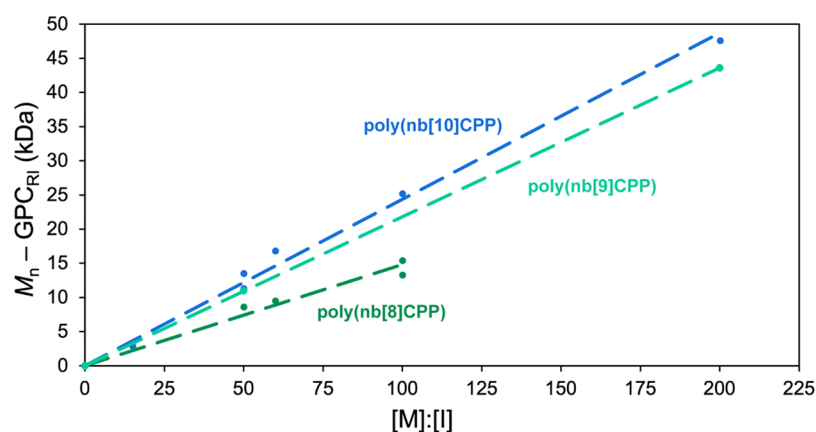


Figure 3. Plot of measured molecular weights (GPC_{RI}) versus monomer-to-initiator ratio for polymerizations conducted with Grubbs G3 in chloroform (data for plot in Table S1).

(Table S1). Due to the highly unusual nature of poly(nbCPP)s, we conducted control experiments with a low molar mass, and acyclic benzonorbornadiene monomer (diMeObnb) to validate our polymerization procedure and to contextualize our molecular weight results. We found that while there was still a moderate difference between theoretical and measured molecular weight values for the model polymer, we consistently achieved low (typically ≤ 1.05) dispersity values (Table S2).

By comparing the model system with the CPP-based polymers, it became apparent that solubility was a critical

factor in the polymerization outcomes. Generally for ROMP, high monomer concentrations are ideal for achieving polymer samples with low dispersity.⁴⁵ CPP derivatives are well-soluble relative to other polyaromatic hydrocarbons, but are certainly less soluble than a typical low-molecular-weight monomer, so we had to decrease the concentration of our reactions accordingly. Particularly with nb[10]CPP, the least soluble of the monomers, some polymerizations did not go to completion—not due to insufficient reaction time, but rather due to a small amount of monomer being deposited on the sides of the flask rather than being in solution. Solubility also

played an important role for analysis of the final polymers. We found that above a certain degree of polymerization (DP), measured molecular weights no longer followed the established trend because of incomplete solubility of the polymer samples (Table S1). Surprisingly, **poly(nb[8]CPP)** had the lowest cutoff for solubility, with samples over DP 100 being noticeably less soluble and DP 200 samples being completely insoluble. Finally, we carried out GPC analysis on select samples using a multiangle light scattering (MALS) detector to obtain more accurate molecular weight values that could serve as a frame of reference for the remaining **poly(nbCPP)** samples. The molecular weights obtained from GPC_{MALS} were notably higher than both the previously measured GPC_{RI} values and the theoretical molecular weights (Table 1).

Table 1. GPC (RI/MALS) Results for Selected Polymer Samples

sample ^a	[M]: [I]	theoretical M_n (g/mol)	M_n – GPC_{RI} (g/mol)	\bar{M}_w – GPC_{RI}	M_n – GPC_{MALS} (g/mol)	\bar{M}_w – GPC_{MALS}
p[8]	50	33,700	8,500	1.18	60,500	1.07
p[8]	100	67,400	13,300	1.23	98,600	1.04
p[9]	50	37,600	10,900	1.22	60,200	1.10
p[10]	50	41,400	13,600	1.19	67,200	1.06
p[10]	100	82,600	25,000	1.22	118,000	1.08
p[10]	200	165,000	48,200	1.56	274,000	1.23

^aIn Table 1 and Table 2, p[8] = **poly(nb[8]CPP)**; p[9] = **poly(nb[9]CPP)**; p[10] = **poly(nb[10]CPP)**.

Interestingly, GPC_{MALS} analysis also indicated lower dispersity values in all cases, and the majority of samples had dispersities less than 1.10. The large divergence between GPC_{MALS} and GPC_{RI} results brings to light the value of acknowledging the limitations of various molecular weight measurement techniques, carefully considering underlying assumptions and avoiding overinterpretation of ambiguous or imperfect results (for instance, placing undue emphasis on low dispersity when clearly it depends on measurement technique). In addition, GPC_{MALS} was used to assess the solution-state conformation of DP 200 **poly(nb[10]CPP)** (other samples were below the limit of detection). The relationship between radius of gyration and molecular weight for this sample (Figure S7) indicated a

dense, sphere-like conformation, a result that could help explain the lower-than-expected molecular weight values obtained from GPC_{RI} . Intrinsic viscosity measurements and subsequent Mark–Houwink analysis also indicated hard-sphere polymer chain conformations ($a < 0.5$) for **poly(nbCPP)s** (Figure S6).⁴⁶

After determining that ROMP of **nbCPPs** proceeds in a controlled manner based on the ability to regulate the molecular weight of polymer samples, we were extremely interested in demonstrating that block copolymers composed of CPP units could be prepared this way. One marker of a “living” polymerization is that polymer chain ends remain active until a terminating agent is added, allowing formation of block copolymers by sequential addition of different types of monomers. We focused our attention on the synthesis of block copolymer **poly(nb[10]CPP-block-[8]CPP)** and statistical copolymer **poly(nb[8]CPP-stat-[10]CPP)** for comparison, both with a 1:1 mol ratio of **nb[8]CPP** and **nb[10]CPP**. **Poly(nb[8]CPP-stat-[10]CPP)** samples were prepared by premixing **nb[8]CPP** with **nb[10]CPP**, then treating the mixture with Grubbs G3. In contrast, to prepare **poly(nb[10]CPP-block-[8]CPP)**, **nb[10]CPP** was first added to a flask and polymerized according to the typical procedure, and then an aliquot was removed from the reaction for analysis, and a solution of **nb[8]CPP** was transferred into the reaction to form the second block (see SI for details). Comparison of ¹H NMR spectra and GPC traces obtained after reaction of the first block and both blocks clearly show that synthesis of the desired block copolymer **poly(nb[10]CPP-block-[8]CPP)** was successful (Figure 4). In the NMR spectrum of **poly(nb[10]CPP-block-[8]CPP)**, an additional peak appears at 7.47 ppm, corresponding to **nb[8]CPP** units. GPC shows the expected increase in molecular weight with minimal change in dispersity after extension of the polymer chains with the second block. NMR and GPC results for **poly(nb[8]CPP-stat-[10]CPP)** (see SI) were similar to the results for **poly(nb[10]CPP-block-[8]CPP)**, indicating that the samples have comparable compositions and molecular weights, as expected, and differ only by sequence of the constituent monomers. MALDI spectra were obtained for some copolymer samples, and while these were again not suitable for determining average molecular weight, they do show differing “fingerprints” for

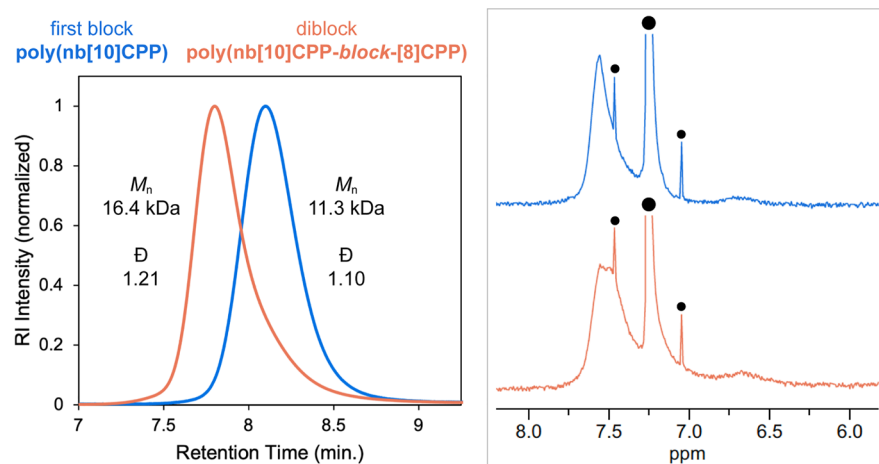


Figure 4. GPC_{RI} (left) and ¹H NMR (right) evidence for formation of **poly(nb[10]CPP-block-[8]CPP)** (data from sample 1, Table S3). $CHCl_3$ and its satellite peaks are marked with circles.

Table 2. Optical Properties of nb[8]CPP, nb[9]CPP, nb[10]CPP, and Selected Polymer Samples

sample	absorbance maximum, solution (nm)	absorbance maximum, solid (nm)	extinction coefficient ($L \cdot mol^{-1} \cdot cm^{-1}$)	emission maximum, solution (nm)	quantum yield, solution (%)	emission maximum, solid (nm)	quantum yield, solid (%)
nb[8]CPP	334	333	$(1.26 \pm 0.06) \times 10^5$	521	22.5 ± 0.6	515	43.1 ± 1.4
p[8] DP 50	332	331	n.d.	527	20.3 ± 0.8	534	2.8 ± 0.3
p[8] DP 200	insoluble	n.d.	insoluble	insoluble	insoluble	536	2.5 ± 0.2
nb[9]CPP	335	334	$(1.29 \pm 0.11) \times 10^5$	483	53.8 ± 0.1	492	36.4 ± 1.4
p[9] DP 50	334	335	n.d.	494	52.4 ± 0.1	496	1.0 ± 0.1
nb[10]CPP	336	329	$(1.46 \pm 0.17) \times 10^5$	465	78.8 ± 0.3	460	34.1 ± 0.3
p[10] DP 50	334	335	n.d.	471	74.8 ± 0.5	482	0.9 ± 0.1
p[10] DP 200	334	335	n.d.	472	75.8 ± 0.6	482	2.7 ± 0.2

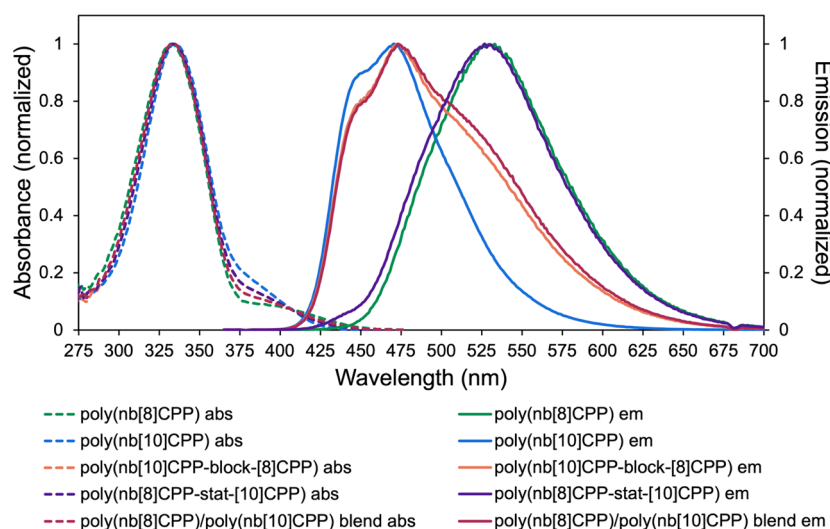


Figure 5. Absorbance (abs) and fluorescence emission (em) spectra of homopolymer and copolymer samples in THF.

block and statistical copolymers (Figure S2). Successful synthesis of **poly(nb[10]CPP-block-[8]CPP)** provides further support for the controlled nature of ROMP of nbCPPs.

Optical Properties of nbCPPs and poly(nbCPP)s. We next used UV–vis absorption and fluorescence spectroscopies to examine the optical properties of nbCPPs and poly(nbCPP)s. We were interested in (1) determining whether the appended norbornenes would alter the properties of nbCPPs relative to unfunctionalized CPPs, (2) assessing the degree to which the optical properties of nbCPPs are retained in poly(nbCPP)s, and (3) comparing optical properties among poly(nbCPP)s with consideration to the additional materials design parameters of polymer composition and sequence. For context, CPPs have an absorbance maximum near 340 nm regardless of nanohoop size, but in contrast to linear paraphenylenes, the emission maxima of CPPs red-shift as the number of phenyl units decreases. For instance, the emission maxima for [10]CPP, [9]CPP, and [8]CPP are 466, 494, and 533 nm, respectively.¹⁷ We found that the common absorption band of CPPs was retained in the norbornene CPP monomers, and fluorescence maxima of the norbornene monomers in solution were nearly identical to those of the parent CPPs (Table 2). Like with the parent CPPs,^{47,48} both

the extinction coefficients and the quantum yields of nbCPPs increase with hoop size, resulting in the larger nanohoops being brighter fluorophores. Although CPPs are bright solids, reports on solid-state fluorescence measurements of these molecules are scarce. The few available examples report much lower quantum yields of CPPs as solids than in solution, except when the CPPs are “diluted” in a polymer matrix.^{49–51} We examined the solid-state fluorescence of **nb[8]CPP**, **nb[9]CPP**, and **nb[10]CPP** and found that the trend in quantum yield reverses compared to the solution results, with **nb[8]CPP** having the highest quantum yield as a solid. The difference among the values also narrows, with all of the monomers exhibiting quantum yields between 0.34 and 0.44, quite high for neat solids (Table 2). In summary, to the extent which we could compare to the literature, the optoelectronic properties of **nb[8]CPP**, **nb[9]CPP**, and **nb[10]CPP** are similar to the properties of [8]CPP, [9]CPP, and [10]CPP, respectively.

All of the polymers share an absorbance maximum near 340 nm—essentially no change from what is observed for nbCPP monomers and underivatized CPPs. The emission maxima for **poly(nb[8]CPP)**, **poly(nb[9]CPP)**, and **poly(nb[10]CPP)** are red-shifted a few nanometers relative to the respective

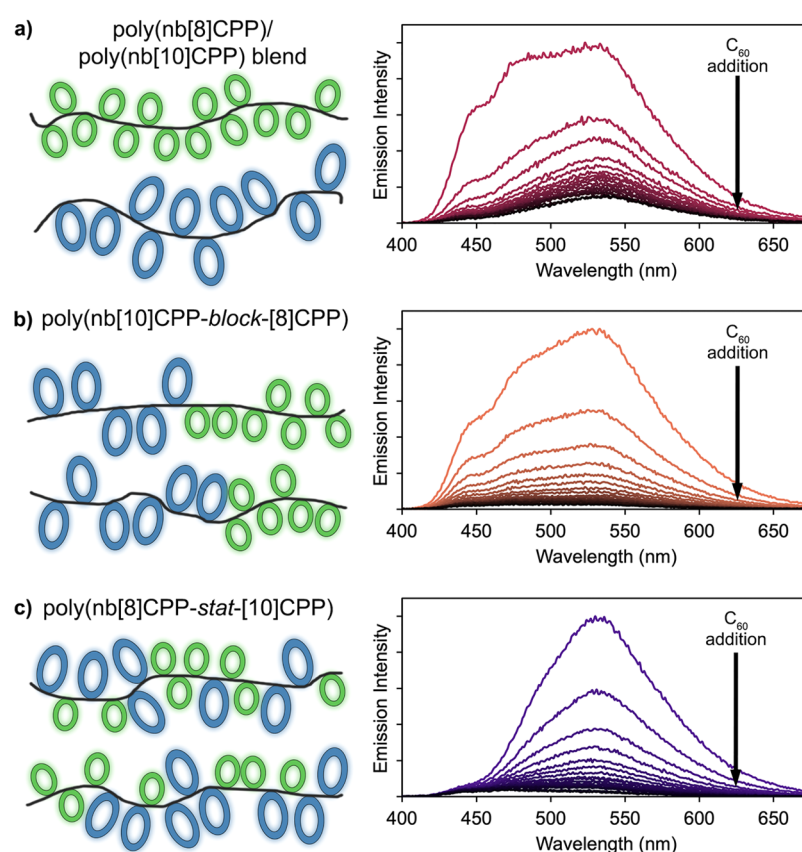


Figure 6. (a) A $\text{poly}(\text{nb}[8]\text{CPP})/\text{poly}(\text{nb}[10]\text{CPP})$ blend, (b) $\text{poly}(\text{nb}[10]\text{CPP}\text{-block-}[8]\text{CPP})$, and (c) $\text{poly}(\text{nb}[8]\text{CPP}\text{-stat-}[10]\text{CPP})$, represented pictorially on the left, exhibit drastically different emission profiles and fluorescence responses to the addition of C_{60} . See SI for experimental details.

monomers in both the solution and the solid state (Table 2, Figure S11, and Figure S12). The quantum yields of the homopolymers in solution closely reflect the results for the respective monomers. The monomers themselves are very bright fluorophores, brighter than many common fluorescent dyes,⁵² so discovering that $\text{poly}(\text{nbCPP})$ s retain a high quantum yield in solution is exciting. These polymers could, for instance, find use as ultrabright fluorescent tags. As solids, however, the polymers have much lower quantum yields (Table 2), indicating that the polymers pack in a way that allows additional modes of nonradiative relaxation not available to the monomers in the solid state. In the case of copolymers, fluorescence emission varies with polymer sequence. $\text{Poly}(\text{nb}[10]\text{CPP}\text{-block-}[8]\text{CPP})$ exhibits emission peaks correlating to both types of monomer units, whereas the emission spectrum of $\text{poly}(\text{nb}[8]\text{CPP}\text{-stat-}[10]\text{CPP})$ appears quite similar to that of $\text{poly}(\text{nb}[8]\text{CPP})$ (Figure 5). We attribute this difference to energy transfer occurring between monomer units in $\text{poly}(\text{nb}[8]\text{CPP}\text{-stat-}[10]\text{CPP})$ but not $\text{poly}(\text{nb}[10]\text{CPP}\text{-block-}[8]\text{CPP})$. Energy transfer between CPPs of different sizes was observed previously in a different system, a heterocatenane composed of [9]CPP and [12]CPP that exhibited a fluorescence emission spectrum closely resembling that of [9]CPP.⁵³ The occurrence of energy transfer between $\text{nb}[10]\text{CPP}$ and $\text{nb}[8]\text{CPP}$ units in statistical but not in block copolymers can be rationalized by considering the distance between the units in each case. Energy transfer only occurs efficiently at distances shorter than the Förster distance, R_0 . Based on the overlap integral for the absorbance spectrum of $\text{nb}[8]\text{CPP}$ and the emission spectrum of

$\text{nb}[10]\text{CPP}$, R_0 for these molecules is around 2.4 nm (Figure S13). There is a much higher likelihood of $\text{nb}[8]\text{CPP}$ and $\text{nb}[10]\text{CPP}$ units being within 2.4 nm of each other in $\text{poly}(\text{nb}[8]\text{CPP}\text{-stat-}[10]\text{CPP})$ compared to $\text{poly}(\text{nb}[10]\text{CPP}\text{-block-}[8]\text{CPP})$. The emission spectrum of $\text{poly}(\text{nb}[10]\text{CPP}\text{-block-}[8]\text{CPP})$ can be replicated by blending samples of $\text{poly}(\text{nb}[8]\text{CPP})$ and $\text{poly}(\text{nb}[10]\text{CPP})$, confirming that by increasing the distance between the two types of CPP units, they each fluoresce independently (Figure 5). Energy transfer still occurs efficiently in statistical copolymers with varied ratios of $\text{nb}[8]\text{CPP}$ and $\text{nb}[10]\text{CPP}$ units, while in block copolymers and polymer blends with different compositions, the relative intensity of the emission peaks changes (Figure S16). Altogether, the optical properties of this set of polymers offer promise for the development of advanced emissive materials. Not only can we obtain CPP-based homopolymers that retain the desirable properties of the constituent fluorophore units, such a high brightness, but we can also access copolymers whose fluorescence can be modulated by altering polymer sequence and composition.

Fluorescence Response of $\text{Poly}(\text{nbCPP})$ s to C_{60} . Lastly, we wanted to evaluate $\text{poly}(\text{nbCPP})$ s as responsive materials using fullerene C_{60} as an illustrative guest molecule. C_{60} is the best-studied guest for CPPs, and its size-selective binding with [10]CPP (and [10]CPP derivatives) is marked by dramatic fluorescence quenching.³² With other sizes of CPPs, C_{60} produces only minor decreases in fluorescence intensity due to dynamic quenching. Before treating polymer samples with C_{60} , we verified that addition of C_{60} nearly completely quenches the fluorescence of $\text{nb}[10]\text{CPP}$ but not $\text{nb}[8]\text{CPP}$

(Figure S18). We then compared the magnitude and nature of fluorescence quenching in homopolymer and copolymer samples (all DP 100). As expected, poly(nb[10]CPP) exhibits similar quenching behavior to nb[10]CPP and [10]CPP, whereas poly(nb[8]CPP) exhibits relatively minor quenching (Figure S18). As a rule, lower concentrations of C₆₀ were needed to produce the same magnitude of quenching in the polymers relative to the monomers, presumably due to higher local concentrations of CPP units. When poly(nb[10]CPP) and poly(nb[8]CPP) were blended, C₆₀ addition resulted in an intermediate degree of quenching, with the greatest quenching occurring between 420 and 500 nm, the region associated with poly(nb[10]CPP) emission (Figure 6). The emission near 530 nm that arises from poly(nb[8]CPP) is diminished but persists. Copolymers poly(nb[8]CPP-stat-[10]CPP) and poly(nb[10]CPP-block-[8]CPP) also quench to an intermediate degree (Figure S17 and Table S5). Surprisingly, however, C₆₀ addition quenches the fluorescence across the entire emission spectra rather than preferentially at lower wavelengths (Figure 6). Further studies on poly(nbCPP) conformation and cooperative binding effects would be needed to completely explain the underlying reasons for the observed quenching behavior. Nevertheless, the range of accessible fluorescence responses in these polymeric materials from simple combinations of just two monomers is impressive.

CONCLUSIONS AND OUTLOOK

In this work, we have introduced nbCPPs as a new monomer scaffold and demonstrated a straightforward approach to preparing CPP-based polymers using ROMP. Importantly, this controlled polymerization method gives access to poly-(nbCPP)s with varying molecular weights which retain the desirable characteristics of CPPs, such as solubility, size-dependent fluorescence, and host–guest interactions.

In contrast to many polymers composed of fluorophores, poly(nbCPP)s fluoresce brightly in solution, making them potential candidates for bright fluorescent tags for imaging applications. Copolymerizing multiple sizes of nbCPPs provides additional avenues to tune the properties of the resultant polymeric materials. The sequence dependence of the emission and supramolecular chemistry of CPP-based copolymers highlights the importance of accessing these structures through a “living” polymerization method. Looking ahead, access to block copolymers from nbCPPs poses exciting prospects for synthesis of new materials, such as poly(nbCPP)s selectively doped with nitrogen atoms and hybrid materials made with a combination of CPP units and other monomers. Block copolymers with CPP units comprising one or more blocks could serve as organic light-emitters with tunable and perhaps even white light emission. Additionally, one could envision a vast array of interesting self-assembled materials prepared from CPP-containing amphiphilic block copolymers. Self-assembly of poly(nbCPP)s could also be used to prepare materials in which fullerenes or metallofullerenes are hosted in specific regions of a material for organic electronic or magnetic applications. Further progress toward these advanced polymeric materials would benefit from additional tools for modeling complex nonbiological macromolecules. Ultimately, poly(nbCPP)s represent a new form of carbon nanomaterial, uniquely positioned at the intersection of precise organic synthesis and macromolecular chemistry.

ASSOCIATED CONTENT

Supporting Information

The Supporting Information is available free of charge at <https://pubs.acs.org/doi/10.1021/acscentsci.1c00345>.

Detailed experimental procedures and characterization (PDF)

Crystallographic data for 2 (CIF)

Crystallographic data for nb[8]CPP (CIF)

Crystallographic data for nb[9]CPP (CIF)

Crystallographic data for nb[10]CPP (CIF)

AUTHOR INFORMATION

Corresponding Author

Ramesh Jasti – Department of Chemistry and Biochemistry and Materials Science Institute and Knight Campus for Accelerating Scientific Impact, University of Oregon, Eugene, Oregon 97403, United States; orcid.org/0000-0002-8606-6339; Email: rjasti@uoregon.edu

Authors

Ruth L. Maust – Department of Chemistry and Biochemistry and Materials Science Institute and Knight Campus for Accelerating Scientific Impact, University of Oregon, Eugene, Oregon 97403, United States; orcid.org/0000-0002-1668-721X

Penghao Li – Department of Chemistry and Biochemistry and Materials Science Institute and Knight Campus for Accelerating Scientific Impact, University of Oregon, Eugene, Oregon 97403, United States; orcid.org/0000-0002-1517-5845

Baihao Shao – Department of Chemistry, Dartmouth College, Hanover, New Hampshire 03755, United States

Sarah M. Zeitler – Department of Chemistry, University of Washington, Seattle, Washington 98195, United States

Peiguan B. Sun – Department of Chemistry and Biochemistry and Materials Science Institute and Knight Campus for Accelerating Scientific Impact, University of Oregon, Eugene, Oregon 97403, United States

Harrison W. Reid – Department of Chemistry and Biochemistry and Materials Science Institute and Knight Campus for Accelerating Scientific Impact, University of Oregon, Eugene, Oregon 97403, United States

Lev N. Zakharov – CAMCOR – Center for Advanced Materials Characterization in Oregon, University of Oregon, Eugene, Oregon 97403, United States

Matthew R. Golder – Department of Chemistry, Molecular Engineering and Science Institute, University of Washington, Seattle, Washington 98195, United States; orcid.org/0000-0001-5848-7366

Complete contact information is available at: <https://pubs.acs.org/doi/10.1021/acscentsci.1c00345>

Author Contributions

All authors have given approval to the final version of the manuscript.

Notes

The authors declare no competing financial interest.

ACKNOWLEDGMENTS

This material is based upon work supported by the U.S. Department of Energy, Office of Science, Office of Basic Energy Sciences under Award Number DE-SC-0019017 and

by the National Science Foundation Graduate Research Fellowship under Grant No. 1309047. The authors thank Dr. Casey Check, Dr. Nanette Jarenwattananon, Hazel Fargher, Dr. Terri Lovell, Dr. Brantly Fulton, Dr. Mike Fortunato, Josh Razink, Tavis Price, Prof. A. J. Boydston, and PolyAnalytik, Inc. for help with software and instrument training and preliminary experiments.

REFERENCES

- (1) Dinadayalane, T. C.; Leszczynski, J. Remarkable Diversity of Carbon-Carbon Bonds: Structures and Properties of Fullerenes, Carbon Nanotubes, and Graphene. *Struct. Chem.* **2010**, *21*, 1155–1169.
- (2) Pinzón, J. R.; Villalta-Cerdas, A.; Echegoyen, L. Fullerenes, Carbon Nanotubes, and Graphene for Molecular Electronics. In *Unimolecular and Supramolecular Electronics I*; Metzger, R. M., Ed.; Springer Berlin Heidelberg: Berlin, Heidelberg, 2012; pp 127–174.
- (3) Lim, S. Y.; Shen, W.; Gao, Z. Carbon Quantum Dots and Their Applications. *Chem. Soc. Rev.* **2015**, *44*, 362–381.
- (4) Segawa, Y.; Levine, D. R.; Itami, K. Topologically Unique Molecular Nanocarbons. *Acc. Chem. Res.* **2019**, *52*, 2760–2767.
- (5) Li, L.; Yan, X. Colloidal Graphene Quantum Dots. *J. Phys. Chem. Lett.* **2010**, *1*, 2572–2576.
- (6) Senese, A. D.; Chalifoux, W. A. Nanographene and Graphene Nanoribbon Synthesis via Alkyne Benzannulations. *Molecules* **2019**, *24*, 118.
- (7) Yang, X.; Dou, X.; Rouhanipour, A.; Zhi, L.; Räder, H. J.; Müllen, K. Two-Dimensional Graphene Nanoribbons. *J. Am. Chem. Soc.* **2008**, *130*, 4216–4217.
- (8) Thomas, S. W.; Joly, G. D.; Swager, T. M. Chemical Sensors Based on Amplifying Fluorescent Conjugated Polymers. *Chem. Rev.* **2007**, *107*, 1339–1386.
- (9) Alvarez, A.; Costa-Fernández, J. M.; Pereiro, R.; Sanz-Medel, A.; Salinas-Castillo, A. Fluorescent Conjugated Polymers for Chemical and Biochemical Sensing. *TrAC, Trends Anal. Chem.* **2011**, *30*, 1513.
- (10) Giacalone, F.; Martín, N. Fullerene Polymers: Synthesis and Properties. *Chem. Rev.* **2006**, *106*, 5136–5190.
- (11) Dawson, R.; Cooper, A. I.; Adams, D. J. Nanoporous Organic Polymer Networks. *Prog. Polym. Sci.* **2012**, *37*, 530–563.
- (12) Von Kugelgen, S.; Piskun, I.; Griffin, J. H.; Eckdahl, C. T.; Jarenwattananon, N. N.; Fischer, F. R. Templated Synthesis of End-Functionalized Graphene Nanoribbons through Living Ring-Opening Alkyne Metathesis Polymerization. *J. Am. Chem. Soc.* **2019**, *141*, 11050–11058.
- (13) Yu, C.; Turner, M. L. Soluble Poly(P-phenylenevinylene)s through Ring-Opening Metathesis Polymerization. *Angew. Chem., Int. Ed.* **2006**, *45*, 7797–7800.
- (14) Elacqua, E.; Gregor, M. Poly(Arylenevinylene)s through Ring-Opening Metathesis Polymerization of an Unsymmetrical Donor-Acceptor Cyclophane. *Angew. Chem., Int. Ed.* **2019**, *58*, 9527–9532.
- (15) Stuparu, M. C. Rationally Designed Polymer Hosts of Fullerene. *Angew. Chem., Int. Ed.* **2013**, *52*, 7786–7790.
- (16) Lawrence, J.; Goto, E.; Ren, J. M.; McDearmon, B.; Kim, D. S.; Ochiai, Y.; Clark, P. G.; Laitar, D.; Higashihara, T.; Hawker, C. J. A Versatile and Efficient Strategy to Discrete Conjugated Oligomers. *J. Am. Chem. Soc.* **2017**, *139*, 13735–13739.
- (17) Darzi, E. R.; Jasti, R. The Dynamic, Size-Dependent Properties of [5]-[12]Cycloparaphenylenes. *Chem. Soc. Rev.* **2015**, *44*, 6401–6410.
- (18) Lovell, T. C.; Colwell, C. E.; Zakharov, L. N.; Jasti, R. Symmetry Breaking and the Turn-on Fluorescence of Small, Highly Strained Carbon Nanohoops. *Chem. Sci.* **2019**, *10*, 3786–3790.
- (19) Darzi, E. R.; Hirst, E. S.; Weber, C. D.; Zakharov, L. N.; Lonergan, M. C.; Jasti, R. Synthesis, Properties, and Design Principles of Donor-Acceptor Nanohoops. *ACS Cent. Sci.* **2015**, *1*, 335–342.
- (20) Chaudhuri, S.; Mohanan, M.; Willems, A. V.; Bertke, J. A.; Gavvalapalli, N. β -Strand Inspired Bifacial π -Conjugated Polymers. *Chem. Sci.* **2019**, *10*, 5976–5982.
- (21) McDearmon, B.; Lim, E.; Lee, I.-H.; Kozycz, L. M.; O'Hara, K.; Robledo, P. I.; Venkatesan, N. R.; Chabiny, M. L.; Hawker, C. J. Effects of Side-Chain Topology on Aggregation of Conjugated Polymers. *Macromolecules* **2018**, *51*, 2580–2590.
- (22) Ball, M.; Zhong, Y.; Fowler, B.; Zhang, B.; Li, P.; Etkin, G.; Paley, D. W.; Decatur, J.; Dalsania, A. K.; Li, H.; et al. Macrocyclization in the Design of Organic N-Type Electronic Materials. *J. Am. Chem. Soc.* **2016**, *138*, 12861–12867.
- (23) Marsella, M. J.; Swager, T. M. Designing Conducting Polymer-Based Sensors: Selective Ionochromic Response in Crown Ether Containing Polythiophenes. *J. Am. Chem. Soc.* **1993**, *115*, 12214–12215.
- (24) Alsbaiie, A.; Smith, B. J.; Xiao, L.; Ling, Y.; Helbling, D. E.; Dichtel, W. R. Rapid Removal of Organic Micropollutants from Water by a Porous β -Cyclodextrin Polymer. *Nature* **2016**, *529*, 190–194.
- (25) Gyanwali, G.; Hikkaduwa Koralege, R. S.; Hodge, M.; Ausman, K. D.; White, J. L. C60-Polymer Nanocomposite Networks Enabled by Guest-Host Properties. *Macromolecules* **2013**, *46*, 6118–6123.
- (26) Wu, Q.; Rauscher, P. M.; Lang, X.; Wojtecki, R. J.; de Pablo, J. J.; Hore, M. J. A.; Rowan, S. J. Poly[n]Catenanes: Synthesis of Molecular Interlocked Chains. *Science* **2017**, *358*, 1434–1439.
- (27) Iwasa, K.; Takashima, Y.; Harada, A. Fast Response Dry-Type Artificial Molecular Muscles with [C2]Daisy Chains. *Nat. Chem.* **2016**, *8*, 625–632.
- (28) Murakami, T.; Schmidt, B. V. K. J.; Brown, H. R.; Hawker, C. J. One-Pot “Click” Fabrication of Slide-Ring Gels. *Macromolecules* **2015**, *48*, 7774–7781.
- (29) Ito, K. Novel Cross-Linking Concept of Polymer Network: Synthesis, Structure, and Properties of Slide-Ring Gels with Freely Movable Junctions. *Polym. J.* **2007**, *39*, 489–499.
- (30) Jasti, R.; Bhattacharjee, J.; Neaton, J. B.; Bertozzi, C. R. Synthesis, Characterization, and Theory of [9]-, [12]-, and [18]-Cycloparaphenylene: Carbon Nanohoop Structures. *J. Am. Chem. Soc.* **2008**, *130*, 17646–17647.
- (31) Mun, J.; Kang, J.; Zheng, Y.; Luo, S.; Wu, H.-C.; Matsuhisa, N.; Xu, J.; Wang, G.-J. N.; Yun, Y.; Xue, G.; et al. Conjugated Carbon Cyclic Nanorings as Additives for Intrinsically Stretchable Semiconducting Polymers. *Adv. Mater.* **2019**, *31*, 1903912.
- (32) Iwamoto, T.; Watanabe, Y.; Sadahiro, T.; Haino, T.; Yamago, S. Size-Selective Encapsulation of C60 by [10]Cycloparaphenylene: Formation of the Shortest Fullerene-Peapod. *Angew. Chem., Int. Ed.* **2011**, *50*, 8342–8344.
- (33) Xu, Y.; von Delius, M. The Supramolecular Chemistry of Strained Carbon Nanohoops. *Angew. Chem., Int. Ed.* **2020**, *59*, 559–573.
- (34) Xia, J.; Bacon, J. W.; Jasti, R. Gram-Scale Synthesis and Crystal Structures of [8]- and [10]CPP, and the Solid-State Structure of C60@[10]CPP. *Chem. Sci.* **2012**, *3*, 3018–3021.
- (35) Van Raden, J. M.; White, B. M.; Zakharov, L. N.; Jasti, R. Nanohoop Rotaxanes from Active Metal Template Syntheses and Their Potential in Sensing Applications. *Angew. Chem., Int. Ed.* **2019**, *58*, 7341–7345.
- (36) Huang, Q.; Zhuang, G.; Zhang, M.; Wang, J.; Wang, S.; Wu, Y.; Yang, S.; Du, P. A Long π -Conjugated Poly(Para-Phenylene)-Based Polymeric Segment of Single-Walled Carbon Nanotubes. *J. Am. Chem. Soc.* **2019**, *141*, 18938–18943.
- (37) Peters, G. M.; Grover, G.; Maust, R. L.; Colwell, C. E.; Bates, H.; Edgell, W. A.; Jasti, R.; Kertesz, M.; Tovar, J. D. Linear and Radial Conjugation in Extended π -Electron Systems. *J. Am. Chem. Soc.* **2020**, *142*, 2293–2300.
- (38) Mai, Y.; Eisenberg, A. Self-Assembly of Block Copolymers. *Chem. Soc. Rev.* **2012**, *41*, 5969–5985.
- (39) Sisto, T. J.; Zakharov, L. N.; White, B. M.; Jasti, R. Towards Pi-Extended Cycloparaphenylenes as Seeds for CNT Growth: Investigating Strain Relieving Ring-Openings and Rearrangements. *Chem. Sci.* **2016**, *7*, 3681–3688.
- (40) Kayahara, E.; Qu, R.; Yamago, S. Bromination of Cycloparaphenylenes: Strain-Induced Site-Selective Bis-Addition and Its

Application for Late-Stage Functionalization. *Angew. Chem., Int. Ed.* **2017**, *56*, 10428–10432.

(41) Slugovc, C. The Ring Opening Metathesis Polymerisation Toolbox. *Macromol. Rapid Commun.* **2004**, *25*, 1283–1297.

(42) Leitgeb, A.; Wappel, J.; Slugovc, C. The ROMP Toolbox Upgraded. *Polymer* **2010**, *51*, 2927–2946.

(43) Choi, T.-L.; Grubbs, R. H. Controlled Living Ring-Opening-Metathesis Polymerization by a Fast-Initiating Ruthenium Catalyst. *Angew. Chem., Int. Ed.* **2003**, *42*, 1743–1746.

(44) Grubbs, R. B.; Grubbs, R. H. 50th Anniversary Perspective: Living Polymerization—Emphasizing the Molecule in Macromolecules. *Macromolecules* **2017**, *50*, 6979–6997.

(45) Bielawski, C. W.; Grubbs, R. H. Living Ring-Opening Metathesis Polymerization. *Prog. Polym. Sci.* **2007**, *32*, 1–29.

(46) Lodge, T. P.; Hiemenz, P. C. *Polymer Chemistry*, 3rd ed.; CRC: Boca Raton, 2020.

(47) Darzi, E. R.; Sisto, T. J.; Jasti, R. Selective Syntheses of [7] - [12]Cycloparaphenylenes Using Orthogonal Suzuki - Miyaura Cross-Coupling Reactions. *J. Org. Chem.* **2012**, *77*, 6624–6628.

(48) Fujitsuka, M.; Cho, D. W.; Iwamoto, T.; Yamago, S.; Majima, T. Size-Dependent Fluorescence Properties of [n]-Cycloparaphenylenes (n = 8–13), Hoop-Shaped π -Conjugated Molecules. *Phys. Chem. Chem. Phys.* **2012**, *14*, 14585–14588.

(49) Segawa, Y.; Fukazawa, A.; Matsuura, S.; Omachi, H.; Yamaguchi, S.; Irle, S.; Itami, K. Combined Experimental and Theoretical Studies on the Photophysical Properties of Cycloparaphenylenes. *Org. Biomol. Chem.* **2012**, *10*, 5979–5984.

(50) Qiu, Z.-L.; Tang, C.; Wang, X.-R.; Ju, Y.-Y.; Chu, K.-S.; Deng, Z.-Y.; Hou, H.; Liu, Y.-M.; Tan, Y.-Z. Tetra-benzothiadiazole-based [12]Cycloparaphenylene with Bright Emission and Its Supramolecular Assembly. *Angew. Chem., Int. Ed.* **2020**, *59*, 20868–20872.

(51) Della Sala, P.; Buccheri, N.; Sanzone, A.; Sassi, M.; Neri, P.; Talotta, C.; Rocco, A.; Pinchetti, V.; Beverina, L.; Brovelli, S.; et al. First Demonstration of the Use of Very Large Stokes Shift Cycloparaphenylenes as Promising Organic Luminophores for Transparent Luminescent Solar Concentrators. *Chem. Commun.* **2019**, *55*, 3160–3163.

(52) Lavis, L. D.; Raines, R. T. Bright Ideas for Chemical Biology. *ACS Chem. Biol.* **2008**, *3*, 142–155.

(53) Segawa, Y.; Kuwayama, M.; Hijikata, Y.; Fushimi, M.; Nishihara, T.; Pirillo, J.; Shirasaki, J.; Kubota, N.; Itami, K. Topological Molecular Nanocarbons: All-Benzene Catenane and Trefoil Knot. *Science* **2019**, *365*, 272–276.